A&A 519, L4 (2010)
DOI: 10.1051/0004-6361/201014719

Astronomy & Astrophysics

Letter to the Editor

Herschel⋆ FIR counterparts of selected Lyα emitters at $z \sim 2.2$

Fast evolution since $z \sim 3$ or missed obscured AGNs?⋆⋆

Á. Bongiovanni[1,2], I. Oteo[1,2], J. Cepa[2,1], A. M. Pérez García[1,2], M. Sánchez-Portal[3], A. Ederoclite[1,2], J. A. L. Aguerri[1,2], E. J. Alfaro[4], B. Altieri[3], P. Andreani[14], M. T. Aparicio-Villegas[4], H. Aussel[15], N. Benítez[4], S. Berta[13], T. Broadhurst[12], J. Cabrera-Caño[5], F. J. Castander[6], A. Cava[1,2], M. Cerviño[4], H. Chulani[1], A. Cimatti[16], D. Cristóbal-Hornillos[4,9], E. Daddi[15], H. Dominguez[17], D. Elbaz[15], A. Fernández-Soto[10], N. Förster Schreiber[13], R. Genzel[13], M. F. Gómez[1], R. M. González Delgado[4], A. Grazian[17], C. Gruppioni[18], J. M. Herreros[1], S. Iglesias Groth[1,2], L. Infante[11], D. Lutz[13], B. Magnelli[13], G. Magdis[15], R. Maiolino[17], I. Márquez[4], V. J. Martínez[7], J. Masegosa[4], M. Moles[4,9], A. Molino[4], R. Nordon[13], A. del Olmo[4], J. Perea[4], A. Poglitsch[13], P. Popesso[13], F. Pozzi[18], F. Prada[4], J. M. Quintana[4], L. Riguccini[15], G. Rodighiero[19], A. Saintonge[13], S. F. Sánchez[8,9], P. Santini[17], L. Shao[13], E. Sturm[13], L. Tacconi[13], and I. Valtchanov[3]

(Affiliations are available on page 5 of the online edition)

Received 2 April 2010 / Accepted 3 August 2010

ABSTRACT

Lyα emitters (LAEs) are seen everywhere in the redshift domain from local to $z \sim 7$. Far-infrared (FIR) counterparts of LAEs at different epochs could provide direct clues on dust content, extinction, and spectral energy distribution (SED) for these galaxies. We search for FIR counterparts of LAEs that are optically detected in the GOODS-North field at redshift $z \sim 2.2$ using data from the *Herschel* Space Telescope with the Photodetector Array Camera and Spectrometer (PACS). The LAE candidates were isolated via color−magnitude diagram using the medium-band photometry from the ALHAMBRA Survey, ancillary data on GOODS-North, and stellar population models. According to the fitting of these spectral synthesis models and FIR/optical diagnostics, most of them seem to be obscured galaxies whose spectra are AGN-dominated. From the analysis of the optical data, we have observed a fraction of AGN or composite over source total number of ∼0.75 in the LAE population at $z \sim 2.2$, which is marginally consistent with the fraction previously observed at $z = 2.25$ and even at low redshift ($0.2 < z < 0.45$), but significantly different from the one observed at redshift ∼3, which could be compatible either with a scenario of rapid change in the AGN fraction between the epochs involved or with a non detection of obscured AGN in other $z = 2$−3 LAE samples due to lack of deep FIR observations. We found three robust FIR (PACS) counterparts at $z \sim 2.2$ in GOODS-North. This demonstrates the possibility of finding dust emission in LAEs even at higher redshifts.

Key words. infrared: galaxies – galaxies: evolution – galaxies: high-redshift

1. Introduction

Lyα emitters (LAEs) are found within the more distant baryonic structures so far detected in the universe. Like most high-redshift objects, they are classified according to the detection technique, a procedure that has generated a wide collection of acronyms (EROs, LBGs, SMG, etc.) that are an indication of our lack of knowledge of the galaxy evolution processes at high redshift. The LAEs can be found at almost any redshift from local (Östlin et al. 2009; Deharveng et al. 2008) through $z \sim 7$ (Bouwens et al. 2009; Iye et al. 2006) and beyond (e.g. Sobral et al. 2009; Bouwens et al. 2010), although LAEs at low redshift (Finkelstein et al. 2009a,d) show quite different properties from those at $z > 2$.

On the high redshift side, LAEs are natural indicators of the reionization of the universe, although the present evidence goes from the early reionization models, which claim that reionization is nearly complete at $z \sim 8$, through the late reionization ones, to end around redshift 6.6 (Choudhury & Ferrara 2006), supported by a number density of LAEs that seem to decrease beyond $z \sim 6$ (Kobayashi et al. 2007). On the low redshift extreme, at $z \sim 2$−3, the relatively scarce number of LAEs detected could be consistent with them being the progenitors of present day L* galaxies. Gawiser et al. (2007) studied a sample of 162 LAEs at $z \sim 3.1$ and found neither evidence of dust obscuration nor a substantial AGN component (of ∼1%) in the host galaxies, which determines that their sample is essentially composed of young, low stellar mass sources without possible far-infrared (FIR) counterparts. These results agree with those obtained by Nilsson et al. (2007), who studied a stacked sample of LAEs at $z = 3.15$. Nevertheless, there is recent evidence about LAEs with different dust contents. For instance, Pirzkal et al. (2007) found dusty but young LAEs at $z \sim 5$. Even more recently, in a study of 170 robust LAE candidates at $z = 2.25$, Nilsson et al. (2009) found a trend of apparent evolution in the LAE properties with respect to their previous work: they detect a significant AGN contribution and red spectral-energy distributions, which imply more massive, dustier, and older galaxies than their *relatives* at $z \gtrsim 3$. This

⋆ *Herschel* is an ESA space observatory with science instruments provided by European-led Principal Investigator consortia and with important participation from NASA.

⋆⋆ Appendices (pages 6 to 9) are only available in electronic form at http://www.aanda.org

result is stressed in Nilsson & Møller (2009), who found that a non-zero fraction of LAEs at $z < 3$ are ULIRGs.

Therefore, for a meaningful fraction of LAEs at $z = 2-3$ it is possible to obtain direct evidence of dust re-emission in FIR produced by the absorption of UV and optical photons from star-forming regions or nuclear activity. Additionally, the Lyα photons are resonantly scattered by neutral hydrogen in the galactic ISM, increasing the probability that they are totally screened. Because of this, Hayes et al. (2010) have recently confirmed that a huge fraction (almost a 90%) of star-forming galaxies emit insufficient Lyα photons to be detected by narrow-band surveys.

Even at higher redshift there is evidence of probably dusty LAEs. Finkelstein et al. (2009b) performed an analysis of the expected detection of dust emission for high-z, narrow-band selected LAEs in GOODS *Chandra* Deep Field-South (CDF-S). Dust in a fraction of $\simeq$0.4 of LAEs with redshift between 4.1 and 5.8 could be detectable in rest-frame wavelengths of 60 and 100 μm. This result is reinforced in Finkelstein et al. (2009c) from a standard SED fitting of LAEs at $z \sim 4.5$ in the same field. Additionally, they propose that the bimodality observed in the age distribution of LAE stellar populations may be owing to dust. With more conservative results, but using a previously developed Lyα/continuum production/transmission model, Dayal et al. (2010) claim to have found an efficient strategy to look for dust emission from LAEs using the new developments of ALMA: they suggest that the Lyα and submillimeter emissions (preferentially in the 850 μm band) for galaxies at $z = (5.7, 6.6;$ FIR in the LAE rest-frame) are correlated and, therefore, a fraction of high-z LAEs (but significantly smaller than the predicted by Finkelstein et al. 2009c) could be observed in the submillimeter regime. This could be supported by the spatial correlation claimed between SMGs and LAEs, where both populations act as high density tracers (Tamura et al. 2009). Thus, AGN fraction, dust contents, and correlation with FIR data would help to provide clues for the evolution of LAEs.

From this brief review, it is clear that the high-z LAE properties are poorly known and on other hand, finding possible counterparts of these objects in the FIR and submillimeter regimes – as we try to demonstrate in this paper – can help to constrain the nature of this apparent duality of LAEs. We present the first results of a multiwavelength analysis of LAE candidates with observations performed with the ESA *Herschel* Space Observatory (Pilbratt et al. 2010) and the PACS instrument (Poglitsch et al. 2010) in the framework of the PACS Evolutionary Probe (PEP, P.I. D. Lutz). The PEP is the *Herschel* Guaranteed Time Key-Project designed to obtain the best profit from *Herschel* instrumentation to study the FIR galaxy population. In our case, only very strong and dusty LAEs could be detected with PACS. Finally, a relative fraction of LAEs hosting AGNs with respect to the overall population is estimated.

Throughout this paper a concordant cosmology with $H_0 = 70\ \mathrm{km\,s^{-1}\,Mpc^{-3}}$ is assumed. Unless otherwise specified, all magnitudes are given in the AB system.

2. Sample selection and ancillary data

2.1. Optical identification of candidate LAEs

We searched for FIR counterparts of LAEs at $z \sim 2.2$ in the northeastern half of the GOODS-North field (~70 sq-arcmin) by using selected filters of the ALHAMBRA system as a part of a more extended study. The Advanced Large Homogeneous Area Medium-Band Redshift Astronomical (ALHAMBRA) survey is aimed at providing a tomography of the evolution of the contents of the universe over most of their cosmic history (see Moles et al. 2008 for a more detailed description of the survey and its scientific goals). This novel approach employs 20 contiguous, equal-width, $FWHM \sim 320$ Å top-hat filters covering from 3500 to 9700 Å plus the Johnson-standard *JHK*s near-infrared (NIR) bands, to observe a total area of 3.5 deg^2 on the sky (a description of the ALHAMBRA photometric system is given in Aparicio Villegas et al. 2010). The observations were carried out with the Calar Alto 3.5 m telescope using the wide-field cameras in the optical, Large Area Imager for Calar Alto (LAICA), and in the NIR, Omega-2000. The magnitude limits achieved by ALHAMBRA are $AB = 25.5$ mag (for an unresolved object, the signal-to-noise ratio $S/N = 5$) in the optical filters from the blue to 8300 Å, and from $AB = 24.7$ to 23.4 for the redder ones. The limits in the NIR are in the Vega system $J \sim 22$ mag, $H \sim 21$ mag, and Ks ~ 20 mag.

The searching procedure adopted is similar to the well-known narrow-band techniques used to find high-redshift galaxies (Cowie & Hu 1998; Gronwall et al. 2007; Ouchi et al. 2008; Shioya et al. 2009; Murayama et al. 2007), but instead of a combination of narrow and broad filters to isolate the line and define the continuum, we used selected ALHAMBRA intermediate bandpass filters for both purposes. Details of the methodology are given in the online Appendix A. Figure 1 shows a detail of the medium-band color−magnitude distribution for our catalog of 2532 spurious-free sources, detected in the northeast fraction of the GOODS-North field. After applying the color- and limiting magnitude selection criteria defined in Appendix A, with an additional 3-σ color−magnitude restriction (dashed line in Fig. 1), we found 134 raw LAE candidates. This gives a mean number density of $\sim 2 \times 10^{-3}$ Mpc^{-3}. However, without spectroscopic information for a statistically significant sample of our raw LAE candidates, these sources were fitted with galaxy templates BC03 (Bruzual & Charlot 2003), using the procedure described in Appendix A to discard the continuum-only objects that show a color excess. Individual fittings also allow us to obtain reliable photometric redshifts and preliminary spectral classifications for the raw LAE candidates. For this purpose, we adopted the photometry from Capak et al. (2004) in the optical (*UBVRIz′*) instead of the ALHAMBRA one. The former data are about 1.1 to 1.5 mag (*AB*) deeper in U, B, V, and R bands than the latter. Not so for the NIR photometry, where ALHAMBRA data are given in the canonical bands. After applying this procedure, we combined the results with an analysis of detection reliability of the Lyα emission line and found 16 secure candidates to LAEs, which are represented in the color−magnitude diagram of Fig. 1 with their corresponding error bars. Optical pseudo-spectra from ALHAMBRA survey and relevant data of these LAEs, including the estimated Lyα luminosity, are given in online Fig. B.1 and Table B.1, respectively.

Additionally, each pseudo-spectrum is complemented with a 3×3 sq-arcsec cutout in z-band from HST-ACS (i.e. close to the UV rest-frame of the source, avoiding possible clumpy features in the far-UV images), when available. With these data we estimated sizes and morphologies of the sources from the isophotal radius (2-σ above background) and fitted one-component Sérsic profiles using `GALFIT` (Peng et al. 2002). In all cases, this approach converged succesfully. The results of this analysis are also included in Table B.1. The LAEs at $z \sim 2.2$ have a mean radius of 1.7 ± 0.4 kpc, except for the objects ALH06146 and ALH07181, which exhibit Sérsic profiles and residuals that suggest the presence of bars and out-of-mean radii. Apart from these two objects, sources in the sample are essentially compact and their Sérsic indexes are consistent with bulge-like galaxies.

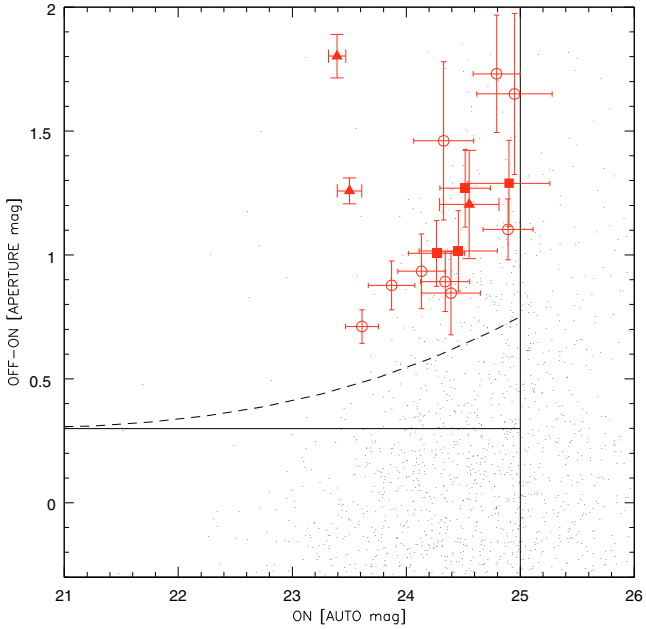

Fig. 1. Diagnostic diagram of the whole catalog and candidates (see online Appendix A for a definition of ON and OFF bands). Continuous lines represent the basic cut in the color OFF-ON and magnitude in the ON-band. Dashed curve indicates the 3-σ color selection threshold, above which the LAE candidates are located. The objects with error bars represent the final sample of LAE candidates: the filled triangles represent LAEs with MIPS (24 μm band) and PACS (100/160 μm bands) counterparts, the filled squares are LAEs with FIR detection in MIPS data only, and the open symbols are the LAEs without FIR counterparts at the sensitivity limit of PEP SDP data.

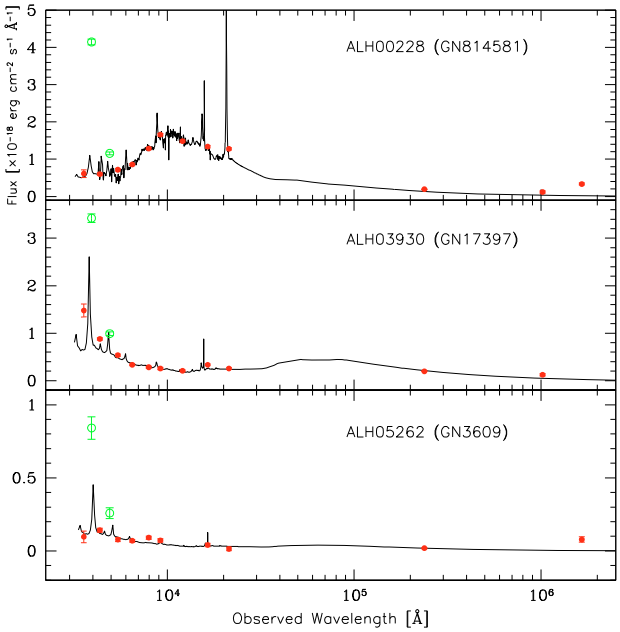

Fig. 2. Best-model fitting of the final LAE candidates at $z \sim 2.2$ with PACS counterparts. SWIRE templates of AGN & composite sources from Polletta et al. (2007) fit the LAE *UBVRIz'* photometry from Capak et al. (2004) and the *JHK*s one from ALHAMBRA (Moles et al. 2008). The red dots represent the photometric data fitted. The open green circles represent the aperture fluxes measured in the ON-band (*A394M* filter, used to account for the redshifted Lyα flux) and through the *A491M* filter (in which wavelength range the redshifted CIVλ1549 line would be contained). The latter values were superposed on the plots, i.e., they were not included in the fitting.

2.2. Matching candidates with FIR data and modeling

We took advantage of the availability of PACS data on the GOODS-North field to search for the counterparts of the final LAE sample in the FIR (100 and 160 μm PACS bands, with a sensitivity of ~5.1 and ~8.7 mJy at 5-σ, respectively) by using the PEP Science Demonstration Phase (SDP) catalog with MIPS-24 μm based position priors (Berta et al. 2010). We performed a match between the catalogs to find which candidates have a detected FIR source closer than 1.5 arcsecs (in the order of the pixel size at 100 μm), and thus study the resulting sample with the aid of spectral synthesis templates from Polletta et al. (2007) for star-forming (SF) and AGN/Composite (AGN/C) objects, but adding the FIR fluxes to the photometric data set previously used. In this preliminary analysis we did not use mid-infrared (MIR) data from *Spitzer*-IRAC because not all the LAE candidates were detected in the raw images. Even so, the IRAC-bands fluxes using ALHAMBRA K_s-band catalog as priors, with the same aperture set, will be included in a forthcoming analysis of PEP data (Oteo et al., in prep.)

We found that seven out of 16 LAEs are detected in MIPS 24 μm band, of which three were also detected at 100 and/or 160 μm bands of PACS. The best-fit for one source of our sample of LAEs with MIPS-24 μm counterparts corresponds to a SF-like template, and the remaining six sources were well fitted with AGN/Composite ones. The LAEs with FIR counterparts in PACS data belong to the latter group, and in the following discussion we only consider those galaxies, unless otherwise specified. The fluxes of the sources in FIR as well as the final spectral classification derived from the best-fitting templates are given in Table B.1. We also distinguished these LAEs in the color−magnitude distribution given in Fig. 1. Likewise, the best-fitted spectra for the LAEs with FIR counterparts in PACS data, corresponding to the objects identified as ALH00228, ALH03930 (with spectroscopic redshift), and ALH05262, are represented in Fig. 2. The best fitting obtained for the first object corresponds to an AGN-1/Composite spectrum, while the other two were fitted using AGN-2/Composite ones. As a consistency test, we compared the $F_\nu(100\ \mu\text{m})/F_\nu(24\ \mu\text{m})$ ratios for the objects ALH00228 and ALH03930 (11.51 ± 3.46 and 11.57 ± 2.31, respectively) with the AGN/SB diagnostic predictions of Mullaney et al. (2010) for PACS filters. These sources fall on the average region (at $z = 2.2$) of AGN composed with SBs.

Finally, we matched the final LAE catalog with the X-ray data of *Chandra*/GOODS-North from Alexander et al. (2003). We found only one counterpart (object ALH08364) in this catalog, whose best-fitted template correspond to AGN/Composite.

3. Results and discussion

We found 134 raw candidates at a mean redshift of 2.2 in the northeastern half of GOODS-North field, using color−magnitude diagnostics of selected medium-band data from ALHAMBRA survey. From this sample, we segregated 16 robust LAEs using spectral synthesis templates. 75% of the final sample were well fitted with AGN/Composite templates, whereas the remaining galaxies were star-forming. Likewise, almost half of the LAEs detected at $z \sim 2.2$ have MIPS 24 μm counterparts (~7.5 μm rest-frame), of which three sources have PACS 100 and/or 160 μm counterparts (~31 and/or 50 μm rest-frame). This proves the possibility of finding dust emission evidence at high redshift, taking into account the sensitivity limits

of the PEP-SDP data (100 μm band: ~5.1 mJy, 5σ). Moreover, using the conversion from MIR to total infrared luminosity of Chary & Elbaz (2001, Eq. (6)), we found that the three brightest counterparts of our LAEs in the 24 μm band are ULIRGs, which partially agree with the main result of Nilsson & Møller (2009) for LAEs at redshifts below $z = 3$. In addition, positive finding of FIR counterparts of spectroscopically observed LAEs has been recently confirmed by our team, using the first data release of PEP Data on the GOODS-South field (Oteo et al., in prep.).

From the analysis of available images of HST-ACS in z-band (rest-frame UV), the LAEs at $z \sim 2.2$ can be described as mainly compact (2 out of 16 of barred morphology), with a typical isophotal radius of ~1.7 kpc. This finding is consistent with the dominant morphology in the LAE sample at $z = 3.1$ analyzed by Bond et al. (2009), but with sizes larger by a factor ~2.

At Lyα luminosity and rest-frame EW limits of 1.95×10^{42} erg s^{-1} and 35 Å, respectively, and under the cosmological assumptions stated in Sect. 1, we compared our LAE sample of possible AGNs with those from recently published data at $z = 2.25$ of Nilsson et al. (2009). To search for possible evolutionary effects on the AGN fraction, we also analyzed the LAE samples of Gronwall et al. (2007) and Ouchi et al. (2008), both at $z = 3.1$. The AGN-to-total fraction for each sample is given in Table B.2. The position of each source of these samples in the previously defined EW-luminosity space is shown in Fig. B.2. From these data it is clear that the AGN fraction increased by a factor of 2.5 (Nilsson et al. 2009) to 15 (this work) between both epochs ($\Delta t \sim 0.9$ Gyr), assuming a mean AGN fraction at $z = 3.1$ of 0.05. This result would suggest a rapid evolution scenario of LAEs classified as AGNs between $z \sim 2$ and 3. Wolf et al. (2003) found a peak in the comoving AGN space density at $z \sim 2$, but our prima facie evidence points to an evolutionary behavior that qualitatively exceeds the one reported by them. Additionally, our AGN-to-total ratio in the LAE population at $z \sim 2.2$ is marginally consistent with that observed at low redshift (of 0.435 at $0.2 < z < 0.45$, Finkelstein et al. 2009a). Note that the AGNs in the samples used for comparison purposes have been classified as such because of the X-ray detection whereas in our case, the lack of detection of FIR counterparts in X-rays (*Chandra*/GOODS-North, Alexander et al. 2003) suggests that these sources are obscured AGNs. Consistently, at $z \sim 2.2$ the FIR emission between 30 to ~110 μm (rest-frame) could be attributed to the re-emission of the dust heated by either the active nucleus or starburst regions close to the nucleus (i.e. a *warm* dust component; Pérez García et al. 1998). If only X-ray detected AGN were considered, the fraction of active nuclei within our sample would be reduced to ~0.16, i.e. compatible with no evolution from the $z \simeq 3.1$ samples.

As an alternative to the presented evolutionary scenario, one could suggest the presence of some kind of selection effect. As shown in Fig. B.2, the sources of our whole LAE sample with $\log L(\mathrm{Ly}\alpha) > 42.5$ have rest-frame EWs a factor of 2−3 higher than the corresponding objects in the sample of Nilsson et al. (2009) at the same redshift. A possible explanation for this effect is that our ON-filter could favor the selection of broad emission-line objects, but this does not clarify the absence of AGNs with rest-frame EWs above ~150 Å in the latter.

This assertion is strengthened by the evidence of the CIVλ1549 redshifted emission line in the ALHAMBRA optical pseudo-spectra of these sources (observed through the filter *A491M*), apart from the photometric signature of the Lyα emission, as shown in Fig. 2. Moreover, the $R-K_s$ colors and $F_\nu(24\ \mu\mathrm{m})/F_\nu(R)$ ratios (see Table B.1) of the FIR counterparts of our LAE sample give preliminary evidence about the degree of obscuration: many of our sources could host moderately to highly obscured AGNs, according to the criteria extensively discussed in Fiore et al. (2008), if the approximation K-band $\approx K_s$ is allowed. Thus, returning to the dicothomy previously raised and apart from the possible evolution of the AGN fraction between redshifts 2 and 3, one might consider that some sources at $z = 2-3$, classified as LAEs by different authors, are also obscured AGNs.

Acknowledgements. This work was supported by the Spanish Plan Nacional de Astrononomía y Astrofísica under grants AYA2008-06311-C02-01 and AYA2006-14056. Based on observations collected at the German-Spanish Astronomical Center, Calar Alto, jointly operated by the Max-Planck-Institut für Astronomie, Heidelberg and the Instituto de Astrofísica de Andalucía (CSIC). PACS has been developed by a consortium of institutes led by MPE (Germany) and including UVIE (Austria); KUL, CSL, IMEC (Belgium); CEA, OAMP (France); MPIA (Germany); IFSI, OAP/AOT, OAA/CAISMI, LENS, SISSA (Italy); IAC (Spain). This development has been supported by the funding agencies BMVIT (Austria), ESA-PRODEX (Belgium), CEA/CNES (France), DLR (Germany), ASI (Italy) and CICYT/MICINN (Spain). We thanks the anonymous referee for valuable comments, which have contributed significatively to the manuscript improvement.

References

Alexander, D. M., Bauer, F. E., Brandt, W. N., et al. 2003, AJ, 126, 539
Aparicio Villegas, T., Alfaro, E. J., Cabrera-Caño, J., et al. 2010, AJ, 139, 1242
Barger, A. J., Cowie, L. L., & Wang, W.-H. 2008, ApJ, 689, 687
Berta, S., Magnelli, B., Lutz, D., et al. 2010, A&A, 518, L30
Bertin, E., & Arnouts, S. 1996, A&AS, 117, 393
Bond, N. A., Gawiser, E., Gronwall, C., et al. 2009, ApJ, 705, 639
Bouwens, R. J., Illingworth, G. D., Bradley, L. D., et al. 2009, ApJ, 690, 1764
Bouwens, R. J., Illingworth, G. D., Oesch, P. A., et al. 2010, ApJ, 709, 133
Bruzual, G., & Charlot, S. 2003, MNRAS, 344, 1000
Capak, P., Cowie, L. L., Hu, E. M., et al. 2004, AJ, 127, 180
Chary, R., & Elbaz, D. 2001, ApJ, 556, 562
Choudhury, T. R., & Ferrara, A. 2006, MNRAS, 371, L55
Cowie, L. L., & Hu, E. M. 1998, AJ, 115, 1319
Dayal, P., Hirashita, H., & Ferrara, A. 2010, MNRAS, 403, 620
Deharveng, J.-M., Small, T., Barlow, T. A., et al. 2008, ApJ, 680, 1072
Finkelstein, S. L., Cohen, S. H., Malhotra, S., et al. 2009a, ApJ, 703, L162
Finkelstein, S. L., Malhotra, S., Rhoads, J. E., Hathi, N. P., & Pirzkal, N. 2009b, MNRAS, 393, 1174
Finkelstein, S. L., Rhoads, J. E., Malhotra, S., & Grogin, N. 2009c, ApJ, 691, 465
Finkelstein, S. L., Cohen, S. H., Malhotra, S., & Rhoads, J. E. 2009d, ApJ, 700, 276
Fiore, F., Grazian, A., Santini, P., et al. 2008, ApJ, 672, 94
Gawiser, E., Francke, H., Lai, K., et al. 2007, ApJ, 671, 278
Gronwall, C., Ciardullo, R., Hickey, T., et al. 2007, ApJ, 667, 79
Guaita, L., Gawiser, E., Padilla, N., et al. 2010, ApJ, 714, 255
Hayes, M., Östlin, G., Schaerer, D., et al. 2010, Nature, 464, 562
Iye, M., Ota, K., Kashikawa, N., et al. 2006, Nature, 443, 186
Kobayashi, M. A. R., Totani, T., & Nagashima, M. 2007, ApJ, 670, 919
Moles, M., Benítez, N., Aguerri, J. A. L., et al. 2008, AJ, 136, 1325
Mullaney, J. R., Alexander, D. M., Huynh, M., Goulding, A. D., & Frayer, D. 2010, MNRAS, 401, 995
Nilsson, K. K., & Møller, P. 2009, A&A, 508, L21
Nilsson, K. K., Møller, P., Möller, O., et al. 2007, A&A, 471, 71
Nilsson, K. K., Pietsch, W., Sala, G., et al. 2009, A&A, 498, 13
Murayama, T., Taniguchi, Y., Scoville, N. Z., et al. 2007, ApJS, 172, 523
Östlin, G., Hayes, M., Kunth, D., et al. 2009, AJ, 138, 923
Ouchi, M., Shimasaku, K., Akiyama, M., et al. 2008, ApJS, 176, 301
Peng, C. Y., Ho, L. C., Impey, C. D., & Rix, H.-W. 2002, AJ, 124, 266
Pérez García, A. M., Rodríguez, E. J. M., & Santolaya, R. E. 1998, ApJ, 500, 685
Pilbratt, G., Riedinger, J. R., Passvogel, T., et al. 2010, A&A, 518, L1
Pirzkal, N., Malhotra, S., Rhoads, J. E., & Xu, C. 2007, ApJ, 667, 49
Polletta, M., Tajer, M., Maraschi, L., et al. 2007, ApJ, 663, 81
Poglitsch, A., Waelkens, C., Geis, N., et al. 2010, A&A, 518, L2
Popesso, P., Dickinson, M., Nonino, M., et al. 2009, A&A, 494, 443
Shioya, Y., Taniguchi, Y., Sasaki, S. S., et al. 2009, ApJ, 696, 546
Sobral, D., Best, P., Geach, J., et al. 2009 [arXiv:0911.4861]
Tamura, Y., Kohno, K., Nakanishi, K., et al. 2009, Nature, 459, 61
Wolf, C., Wisotzki, L., Borch, A., et al. 2003, A&A, 408, 499

[1] Instituto de Astrofísica de Canarias (IAC), 38200 La Laguna, Tenerife, Spain
e-mail: bongio@iac.es
[2] Departamento de Astrofísica, Universidad de La Laguna (ULL), 38205 La Laguna, Tenerife, Spain
[3] Herschel Science Centre (ESAC). Villafranca del Castillo, Spain
[4] Instituto de Astrofísica de Andalucía (CSIC), Granada, Spain
[5] Departamento de Física Atómica, Molecular y Nuclear, Facultad de Física, Universidad de Sevilla, Spain
[6] Institut de Ciències de l'Espai (CSIC), Barcelona, Spain
[7] Departament d'Astronomía i Astrofísica, Universitat de València, València, Spain
[8] Centro Astronómico Hispano-Alemán, Almería, Spain
[9] Centro de Estudios de Física del Cosmos de Aragón, CEFCA, 44001 Teruel, Spain
[10] Instituto de Física de Cantabria (CSIC-UC), 39005 Santander, Spain
[11] Departamento de Astronomía, Pontificia Universidad Católica, Santiago, Chile
[12] School of Physics and Astronomy, Tel Aviv University, Israel
[13] Max-Planck-Institut für Extraterrestrische Physik (MPE), Postfach 1312, 85741 Garching, Germany
[14] ESO, Karl-Schwarzschild-Str. 2, 85748 Garching, Germany
[15] Laboratoire AIM, CEA/DSM-CNRS-Université Paris Diderot, IRFU/Service d'Astrophysique, Bât. 709, CEA-Saclay, 91191 Gif-sur-Yvette Cedex, France
[16] Dipartimento di Astronomia, Università di Bologna, via Ranzani 1, 40127 Bologna, Italy
[17] INAF – Osservatorio Astronomico di Roma, via di Frascati 33, 00040 Monte Porzio Catone, Italy
[18] INAF – Osservatorio Astronomico di Bologna, via Ranzani 1, 40127 Bologna, Italy
[19] Dipartimento di Astronomia, Università di Padova, Vicolo dell'Osservatorio 3, 35122 Padova, Italy

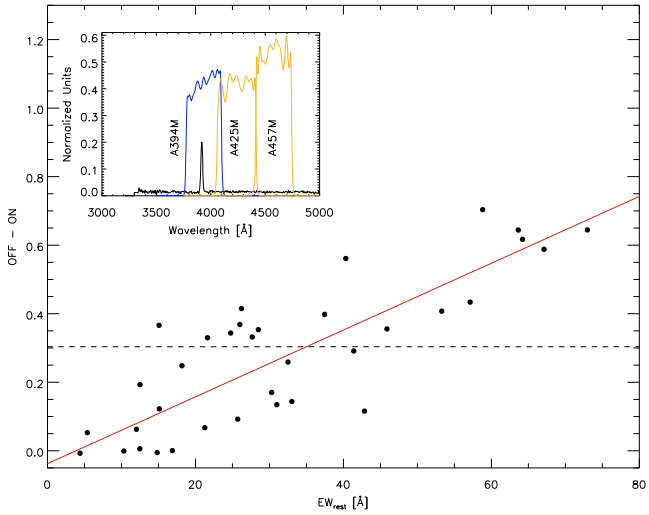

Fig. A.1. ALHAMBRA expected OFF-ON color of the VIMOS LAEs spectra at $z \sim 3$, shifted to $z = 2$, as a function of their equivalent widths. The relation between both variables allows us to have a color selection criterion. The dashed line represents the basic color threshold which corresponds to a $EW_{\rm rest} = 35$ Å. Inset: Bandpasses of the filters used to find LAEs at $2.1 < z < 2.37$. The curves represent the ON (*A394M*) and OFF (*A425M+A457M*) filters transmissions, multiplied by the detector quantum efficiency and the atmospheric transmission at airmass = 1. A typical spectrum of a LAE at $z = 2.2$ is overlaid to show the basis of the photometric selection criterium.

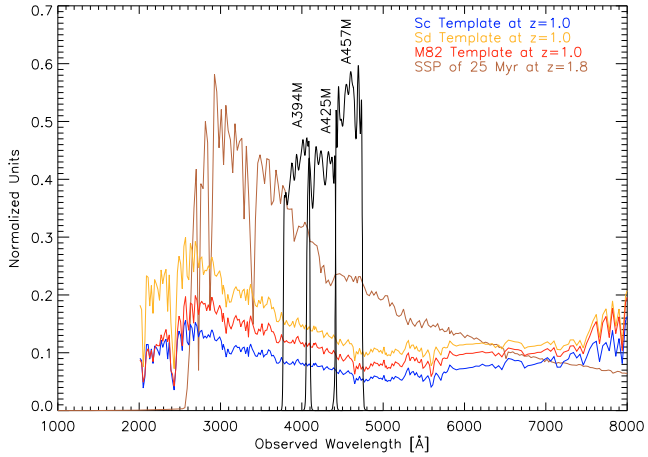

Fig. A.2. Spectra of possible contaminants. The transmission curves of the filter set used to select LAEs and spectra of possible contaminants at different redshifts, built from BC03 and SWIRE templates, are shown. The main contaminants are those whose UV continuum slope is sampled by the filters, resulting in the appearance of false-positive candidates. For the sake of clarity, the spectra and the transmission of the filters have been scaled.

Appendix A: Photometric selection of $z \sim 2.2$ LAE candidates from ALHAMBRA survey in GOODS-North

The method used for finding LAEs is based on a color−magnitude diagnostic diagram. The filter which samples the emission line is the ON filter and those used to define the continuum constitute the OFF filters set. The choice of the ON filter determines the range where the redshifts of the candidates will be. In this way, we seleted the LAE candidates at $2.10 < z < 2.37$ by using the filters *A394M* as ON filter (owing to the official naming of ALHAMBRA filters, the number between letters gives the rounded central wavelength in nanometers; the last letter is the acronym of "Medium" bandpass), and a sum of *A425M* and *A457M* as OFF filters, in order to increase the S/N in the continuum. Figure A.1 (inset) shows the transmission curve of the chosen filters for LAE selection. Assuming an effective filter width equal to its *FWHM*, and taking into account the sky area surveyed, as well as the emission line of interest, we have explored in this way a comoving volume of about 6.63×10^4 Mpc^3.

Once the ON and OFF filters were chosen, and according with the ALHAMBRA survey sensitivity, we adopt a limiting magnitude of 25.0 in the ON-band. Then, we elaborated a color selection criterion to find LAEs as efficiently as possible. We used the data from the GOODS/VIMOS Spectroscopy DR 2.0.1 (Popesso et al. 2009) to simulate the behavior of the SED from a typical LAE against the selected ALHAMBRA filters. From the whole spectroscopic catalog we selected the objects that show a line which corresponds to a Lyα emission. Then the spectra were de-redshifted so that the central wavelength of the lines were within the transmission range of the ON filter in each case, as shown in the example of Fig. A.1, and their rest frame equivalent widths were calculated. After this we were able to compute the OFF-ON color by convolution of the filter profiles with each spectrum. In Fig. A.1 we represent this color against the rest frame equivalent width of the lines, measured with `splot` in `IRAF`. As can be seen, there exists a relation between both variables, which allows us to define a color selection criterion. Our LAE candidates were selected to have rest-frame equivalent widths $EW_{\rm rest} \gtrsim 35$ Å. According to Fig. A.1, this value corresponds to a threshold color of approximately 0.3 for both filter pairs. But taking into account the photometric errors, our adopted color selection criterion is $m_{\rm OFF} - m_{\rm ON} - 0.3 \geq 3\sqrt{\sigma^2_{\rm OFF} + \sigma^2_{\rm ON}}$. This translates the minimum rest-frame equivalent width to $EW_{\rm rest} \gtrsim 35$ Å at the limiting magnitude in the ON-band, corresponding to Lyα luminosities of $\log L = 42.29$ erg s^{-1} at $z = 2.2$.

All photometric measures were performed with `SExtractor` (Bertin & Arnouts 1996) on the full processed and stacked images of the field ALHAMBRA-5, pointing 1. To calculate the color we used three arcsec aperture magnitudes and MAG_AUTO ones to plot the magnitudes of the objects. Sources with `SExtractor` nonzero flags were discarded.

In order to study the nature of the possible continuum contaminants we carried out simulations with galaxy templates of BC03 (Bruzual & Charlot 2003) and SWIRE (Polletta et al. 2007). We took all the templates and redshifted them from $z = 0$ to 3 in bins of $\Delta z = 0.05$. We calculated their expected color and checked whether they satisfy the color selection criterion. As a result, we found that the contaminants appear to be mainly starburst galaxies at $1.0 \lesssim z \lesssim 2.0$, whose UV rest-frame drop is sampled with the filters. As an example, Fig. A.2 shows a set of spectra of different starburst templates that satisfy the color criterium, although they are false positive candidates. More details of this study are included in a forthcoming paper (Oteo et al., in prep.).

Appendix B: Data of $z \sim 2.2$ LAE candidates in GOODS-North

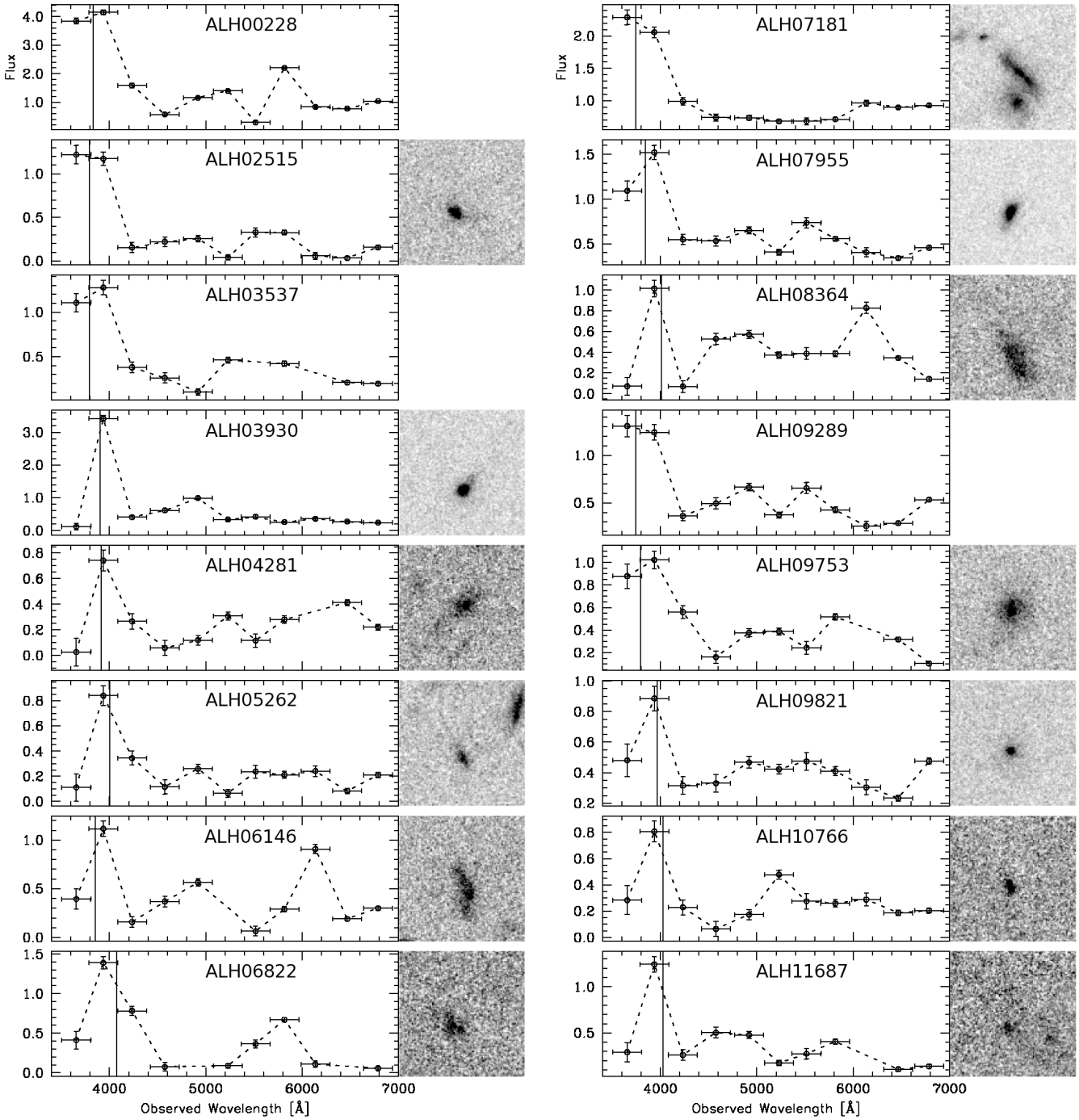

Fig. B.1. Optical pseudo-spectra of $z \sim 2.2$ LAE candidates from ALHAMBRA survey. ACS cutouts (3×3 sq-arcsec) of the objects, when available, are shown in the right side of each pseudo-spectrum. Vertical line inside each panel represent the position of Lyα emission line center at the corresponding photometric or spectroscopic redshift given in Table B.1. Fluxes are in 10^{-18} erg cm^{-2} s^{-1} Å^{-1} units. The horizontal bars represent the effective widths of ALHAMBRA filters. Assumming a concordant cosmology, with $H_0 = 70$ km s^{-1} Mpc^{-3}, the mean scale of the images is ~8.2 kpc arcsec^{-1}.

Table B.1. Combined data list of $z \sim 2.2$ LAE candidates in the north-east half of the GOODS-North field.

[1] ID	RA	Dec	[2] z_{phot}	[3] z_{spec}	[4] $EW(\mathrm{Ly}\alpha)_{rest}$	[5] OFF-ON	[6] ON	[7] log $L(\mathrm{Ly}\alpha)$	[8] $F_{24\,\mu m}$	[9] $F_{100\,\mu m}$	[10] $F_{160\,\mu m}$	[11] $R_{isoph.}$	[12] n	[13] $R - K_s$	[14] $F_\nu(24\,\mu m)/F_\nu(R)$	[15] Sp. T.
ALH00228	12:37:36.1	+62:10:58	2.15	–	159.50 ± 14.36	1.259 ± 0.052	23.502 ± 0.108	43.02	0.192 ± 0.005	0.120 ± 0.031	0.336 ± 0.029	–	–	3.33 ± 0.06	77.38 ± 2.45	AGN/C
ALH02515	12:37:34.3	+62:13:21	2.12	–	274.96 ± 23.21	1.731 ± 0.237	24.793 ± 0.206	42.79	–	–	–	1.92	3.8	4.08 ± 0.07	–	AGN/C
ALH03537	12:38:04.4	+62:14:26	2.12	–	161.72 ± 14.52	1.270 ± 0.157	24.517 ± 0.222	42.61	0.013 ± 0.003	–	–	–	–	4.96 ± 0.06	15.48 ± 3.94	AGN/C
ALH03930	12:37:04.3	+62:14:47	2.13	2.21	297.24 ± 24.94	1.802 ± 0.088	23.393 ± 0.076	43.40	0.198 ± 0.003	0.124 ± 0.023	–	1.79	1.9	5.08 ± 0.06	517.75 ± 45.69	AGN/C
ALH04281	12:37:52.6	+62:15:07	2.22	–	202.84 ± 17.66	1.461 ± 0.319	24.328 ± 0.263	42.86	–	–	–	1.70	1.9	3.91 ± 0.07	–	AGN/C
ALH05262	12:37:48.3	+62:16:10	2.29	–	149.09 ± 13.57	1.204 ± 0.219	24.552 ± 0.261	42.63	0.019 ± 0.003	–	0.079 ± 0.018	1.32	1.4	3.23 ± 0.14	174.82 ± 39.80	AGN/C
ALH06146	12:37:14.9	+62:17:00	2.17	2.13	165.52 ± 14.81	1.289 ± 0.174	24.901 ± 0.359	42.49	0.014 ± 0.003	–	–	0.64	0.8	4.32 ± 0.07	48.95 ± 12.63	AGN/C
ALH06822	12:37:43.2	+62:17:46	2.35	–	131.25 ± 12.23	1.103 ± 0.122	24.893 ± 0.219	42.44	–	–	–	1.04	1.2	2.24 ± 0.16	–	SF
ALH07181	12:37:30.7	+62:18:05	2.08	–	75.64 ± 8.17	0.712 ± 0.068	23.612 ± 0.144	42.46	–	–	–	4.98	0.7	4.87 ± 0.03	–	AGN/C
ALH07955	12:37:26.1	+62:18:57	2.16	–	96.76 ± 9.68	0.877 ± 0.099	23.872 ± 0.205	42.57	–	–	–	2.74	1.2	4.26 ± 0.05	–	SF
ALH08364	12:37:02.1	+62:19:25	2.30	–	117.16 ± 11.18	1.017 ± 0.163	24.456 ± 0.343	42.53	0.037 ± 0.003	–	–	1.78	0.7	3.97 ± 0.06	72.09 ± 8.56	AGN/C
ALH09289	12:37:41.6	+62:20:28	2.08	–	98.82 ± 9.83	0.892 ± 0.120	24.341 ± 0.216	42.36	–	–	–	–	–	–	–	AGN/C
ALH09753	12:37:34.3	+62:20:56	2.12	–	104.77 ± 10.27	0.934 ± 0.151	24.133 ± 0.208	42.50	–	–	–	1.85	1.7	4.50 ± 0.06	–	AGN/C
ALH09821	12:37:42.4	+62:21:02	2.26	–	92.53 ± 9.37	0.846 ± 0.168	24.393 ± 0.258	42.38	–	–	–	1.66	7.6	5.03 ± 0.06	–	SF
ALH10766	12:37:36.4	+62:22:01	2.28	–	251.40 ± 21.39	1.649 ± 0.325	24.949 ± 0.331	42.76	–	–	–	1.49	1.2	–	–	SF
ALH11687	12:37:18.4	+62:23:00	2.31	–	115.63 ± 11.07	1.007 ± 0.132	24.266 ± 0.247	42.60	0.256 ± 0.004	–	–	0.89	1.8	3.81 ± 0.09	670.84 ± 62.20	AGN/C

Notes. [(1)] ID from ALHAMBRA survey data.
[(2)] Photometric redshift.
[(3)] Spectroscopic redshift from Barger et al. (2008).
[(4)] Rest-frame equivalent width (Å) of Lyα emission line from OFF-ON color and relation in Fig. A.1.
[(5)] OFF-ON color.
[(6)] ON-band magnitude.
[(7)] Logarithm of Lyα luminosity (erg s^{-1}).
[(8)] Wavelength flux density in 24 μm band from MIPS ($\times 10^{-18}$ erg cm^{-2} s^{-1} Å^{-1}).
[(9)] Wavelength flux density in 100 μm band from HERSCHEL-PACS ($\times 10^{-18}$ erg cm^{-2} s^{-1} Å^{-1}).
[(10)] Wavelength flux density in 160 μm band from HERSCHEL-PACS ($\times 10^{-18}$ erg cm^{-2} s^{-1} Å^{-1}).
[(11)] Isophotal (2-σ) radius in kpc.
[(12)] Sérsic index.
[(13)] Observed $R - K_s$ color.
[(14)] Ratio of 24 μm to R-band frequency flux densities.
[(15)] Spectral type from templates of Polletta et al. 2007: star-forming (SF) or AGN/Composite (AGN/C).

Table B.2. Number counts of LAEs redshifts 2.2 and 3.1, limited in Lyα luminosity and rest-frame *EW*.

Reference	Mean redshift	Total number	AGN-to-total fraction
Gronwall et al. (2007)	3.1	64	0.016[1]
Ouchi et al. (2008)	3.1	40	0.075[1]
Nilsson et al. (2009)	2.25	73	0.123[1]
This work	2.2	16	0.75[2]

Notes. Only one AGN out of the six observed in this work is detected in X-rays (see main text).
(1) X-ray selected sample.
(2) SED selected sample.

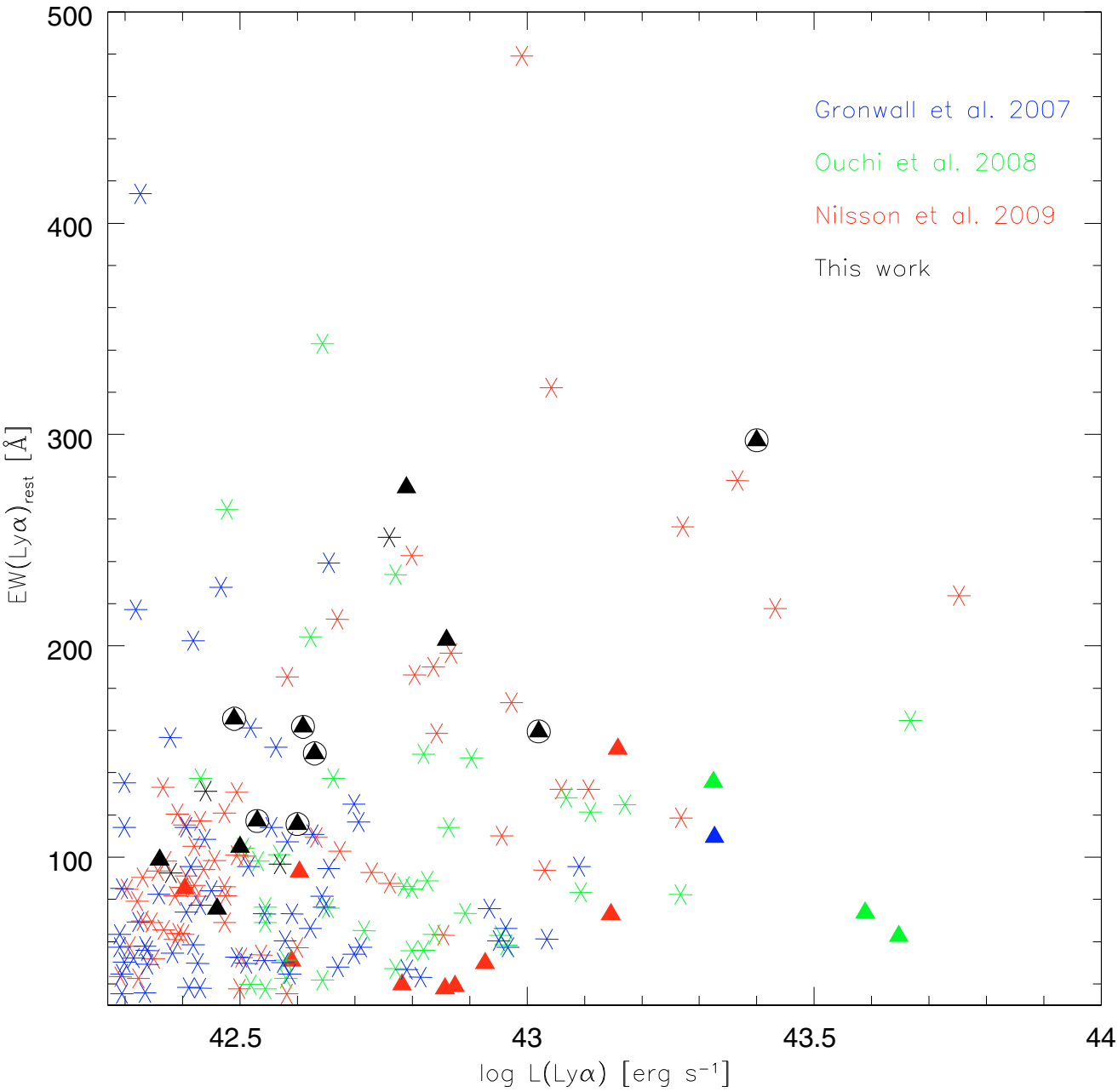

Fig. B.2. Rest-frame EW against Lyα luminosity for the LAE samples referred in Table B.2. Star-forming like LAEs are represented by stars and the AGNs (or AGN/Composite objects) by triangles. Circled triangles are LAEs with FIR counterparts from this work. An interpretation of the AGN distribution in this diagram is given in the main text.